

Correlating Proton Transfer Dynamics To Probe Location in Confined Environments

Myles Sedgwick, Richard L. Cole,[†] Christopher D. Rithner, Debbie C. Crans, and Nancy E. Levinger*

Department of Chemistry, Colorado State University, Fort Collins, Colorado 80523-1872, United States

S Supporting Information

ABSTRACT: The dramatic impact of differing environments on proton transfer dynamics of the photoacid HPTS prompted us to investigate these systems with two highly complementary methods: ultrafast time-resolved transient absorption and two-dimensional NMR spectroscopies. Both ultrafast time-resolved transient absorption spectroscopy and time-resolved anisotropy decays demonstrate the proton transfer dynamics depend intimately on the specific reverse micellar system. For $w_0 = 10$ reverse micelles formed with anionic AOT surfactant, the HPTS proton transfer dynamics are similar to dynamics in bulk aqueous solution, and the corresponding ¹H 2D NOESY NMR spectra display no cross peaks between HPTS and AOT consistent with the HPTS residing well hydrated by water in the interior of the reverse micelle water pool. In contrast, ultrafast transient absorption experiments show no evidence for HPTS photoinduced proton transfer reaction in reverse micelles formed with the cationic CTAB surfactant. In CTAB reverse micelles, clear cross peaks between HPTS and CTAB in the 2D NMR spectra show that HPTS embeds in the interface. These results indicate that the environment strongly impacts the proton transfer reaction and that complementary experimental techniques develop understanding of how location critically affects molecular responses.

Proton transfer reactions are ubiquitous in chemistry, biology and physics.¹ Proton motion is essential to fuel cell operation² and enzymatic function.³ Proton channels shuttle protons across membranes.⁴ Detailed studies of proton transfer in a diverse range of model systems has dramatically increased understanding about fundamental proton transfer dynamics.^{5–8} Studies enlisting the photoacid, 8-hydroxypyrene-1,3,6-trisulfonate (HPTS), Figure 1, have elucidated mechanisms for proton transfer and the role of environment on proton transfer dynamics.^{1,5–7,9–15}

As a photoacid, HPTS has a much lower pK_a in its first electronic excited state (0.5–1.4) than in its ground state (7.2–7.7).^{9,10} In aqueous environments with $pH > pK_a^*$, photo-excitation leads to excited state HPTS deprotonation.¹¹ The significant changes in its electronic absorption and emission spectra (Supporting Information, Figure S1) and its high solubility in aqueous environments contribute to the molecule's utility to study proton transfer reactions. Most HPTS proton transfer studies utilize water as a proton acceptor. Absorption and fluorescence spectroscopy of HPTS in nonaqueous

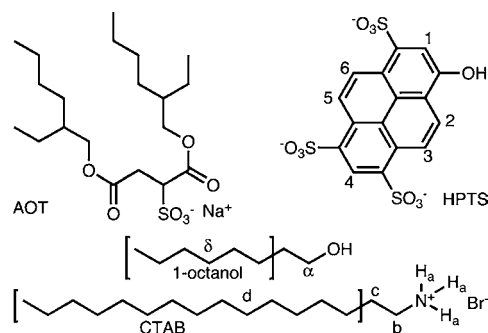


Figure 1. Chemical structures for surfactants AOT and CTAB, cosurfactant 1-octanol, and photoacid HPTS with numbering/lettering for NMR identification.

environments lacking proton acceptors show no proton transfer.^{11,16}

HPTS proton transfer dynamics have been measured in many different systems. Cox et al. measured how ionic strength affected proton transfer of HPTS in aqueous solution.¹⁵ Exploring peptide-based hydrogels Amdursky et al. found that the walls of self-assembled peptide nanotubes affected the proton geminate recombination process.¹⁴ Spry et al. studied HPTS finding proton transfer dynamics in Nafion membranes at high hydration mirrored 0.5 M HCl solution;⁵ at lower hydration levels, the HPTS resides at the Nafion surface where the low local pH precluded proton dissociation. Oxidized porous silicon appears to enhance HPTS proton transfer dynamics.¹⁷ Researchers have also probed proton transfer dynamics at micelle surfaces.^{12,18,19} Roy et al.¹² noted HPTS fluorescence quenching at alkyltrimethylammonium bromide micelle surfaces by acetate counterions. Clearly, complex environments dramatically affect HPTS dynamics.

Researchers have studied nanosized systems to learn about proton transfer in complex, confined and interfacial environments.¹ Isolated water droplets sequestered from a bulk nonpolar phase by a surfactant layer in reverse micelles (RMs) present a versatile model system to explore interfacial and confined environments effects on proton transfer.²⁰ RMs can be prepared from anionic,²¹ cationic,²² nonionic²³ and zwitterionic²⁴ surfactants; their sizes are well-known and proportional to $w_0 = [H_2O]/[surfactant]$.²¹ Using time-resolved emission spectroscopy, Tielrooij et al. showed decreasing HPTS proton transfer rates in anionic AOT and

Received: May 10, 2012

Published: July 5, 2012

nonionic Brij-30 RMs⁶ with decreasing RM size, regardless of the surfactant used. They also reported some HPTS molecules exhibited nonradiative decay, suggesting that the environment prevented proton transfer. Spry et al. also explored HPTS dynamics in AOT RMs finding that proton diffusion decreases dramatically with decreasing w_0 , which they attributed to a change in the water hydrogen bonding network with decreasing micelle size.²⁵ Here we report on HPTS in RMs formed using two common surfactants, the anionic AOT (sodium docusate) in cyclohexane, and the cationic cetyl trimethylammonium bromide (CTAB) with 1-octanol cosurfactant (5:1 ROH/CTAB) in cyclohexane. We compare and contrast results using $w_0 = 10$ RMs for both systems. Details appear in Supporting Information.

Knowledge of a probe's local environment provides critical understanding of proton transfer dynamics. Probe molecule motion depends on local environment thus measurements of molecular rotation through time-resolved anisotropy have become a standard tool in the ultrafast spectroscopy community. Comparison of parallel and perpendicular time-dependent signals for spectroscopic transitions where the transition dipole remains fixed yields the anisotropy decay,²⁶

$$r(t) = \frac{I_{\parallel}(t) - I_{\perp}(t)}{I_{\parallel}(t) + I_{\perp}(t)} = 0.4C_2(t) \quad (1)$$

where $I_{\parallel}(t)$ and $I_{\perp}(t)$ are the time dependent intensities for the probe polarization parallel and perpendicular to the pump and $C_2(t)$ is the second Legendre polynomial. Time-resolved anisotropy has shown that some RM environments^{5,6} reduce HPTS rotational freedom compared to bulk aqueous solution.¹³ Although time-resolved anisotropy shows reduced rotational motion it does not indicate the cause, precluding direct correlation of the reduced molecular motion with changes in the observed proton transfer dynamics. For example, changes in the local viscosity at an interface or embedding the probe molecule in the interface both lead to reduced rotational motion, but it is unclear how these changes would affect the proton transfer reaction.

Using two complementary techniques, we explored the proton transfer dynamics and the location of HPTS in RM environments. Broadband ultrafast time-resolved transient absorption spectroscopy demonstrates significant dependence of the proton transfer dynamics on the charge of surfactant used to form the RMs. The results from 2D NMR measurements show strong interactions of HPTS with the surfactant with a cationic headgroup in the RM while the anionic RM shows no probe-surfactant interactions. Together with time-resolved anisotropy measurements, these studies develop a comprehensive picture of the environmental effect on the HPTS proton transfer dynamics.

Broadband ultrafast time-resolved transient absorption spectra were measured for HPTS in AOT and CTAB RMs as well as in bulk aqueous solution. A detailed description of the spectrometer, data collection and analysis has been reported and a short description appears in Supporting Information.²⁷ Briefly, a 400 nm light pulse excites the HPTS molecule, which is subsequently probed by a delayed white light continuum pulse; complete spectra are collected following photoexcitation. Modulating the pump beam reveals the change of absorption. Spectrograms reflecting changes in intensity as a function of time and wavelength were collected for pump beam polar-

izations both parallel and perpendicular to the probe beam polarization.

Figure 2 shows transient absorption data for HPTS in aqueous solution, and in AOT and CTAB RMs. In aqueous

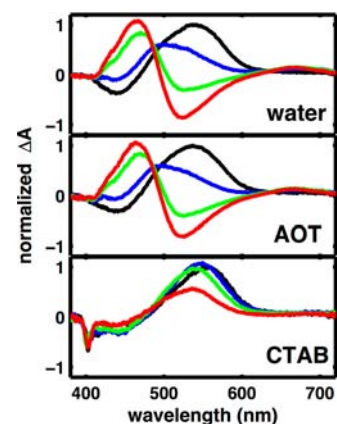


Figure 2. Broadband ultrafast transient spectral traces for HPTS in bulk aqueous solution (top), AOT (middle) and CTAB (bottom) RMs with $w_0 = 10$ for delay times equal to 600 fs (black), 10 ps (blue), 100 ps (green), 1 ns (red). $\Delta A > 0$ represents increased absorption; $\Delta A < 0$ represents bleach or stimulated emission.

solution (top panel) the onset of increased absorption between 500 and 600 nm marks the deprotonation of the molecule. The HPTS dynamics in $w_0 = 10$ AOT RMs are nearly indistinguishable from the response in bulk water, Figure 2, middle and top panels, respectively. In contrast, the transient spectra of HPTS in large CTAB RMs, $w_0 = 10$, Figure 2 bottom, show no spectral shifting or evidence for dye deprotonation. The environment of HPTS in CTAB RMs appears to block proton dissociation.

Figure 3 shows the time-dependent anisotropy signals measuring HPTS molecular reorientation dynamics inside

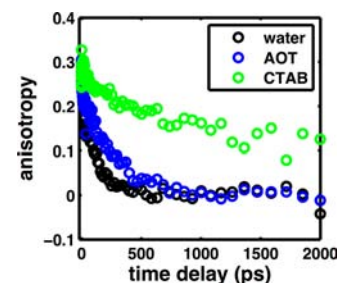


Figure 3. Time-resolved anisotropy decays for HPTS in bulk aqueous solution (black dots), AOT RMs $w_0 = 10$ (blue dots) and CTAB RMs $w_0 = 10$ (green dots). The $r(0) < 0.4$ for all traces due to cancellation from overlap in the excited state absorption and stimulated emission bands at $t = 0$.

CTAB and AOT RMs and in bulk aqueous solution. The HPTS anisotropy decays much more slowly in CTAB RMs than in bulk aqueous solution or in AOT RMs. The signals appear to plateau indicating that the rotational diffusion is incomplete on the experimental time scale. A wobbling-in-a-cone analysis (see Supporting Information) reveals that the HPTS molecule is confined to a cone angle of $\sim 22^\circ$. Although slightly slower than bulk aqueous solution, the HPTS

reorientation in the AOT RMs closely resembles that observed in the bulk aqueous solution.

Various explanations can account for the differences in dynamics observed for HPTS in AOT and CTAB RMs. The slow anisotropy decay times and missing proton transfer signal from HPTS in CTAB RMs vs the fast reorientational decay times and proton transfer dynamics similar to bulk water for AOT suggest HPTS samples significantly different environments in these systems. Time-resolved spectroscopy only indicates dramatically different dynamics, but 2D NMR spectroscopy allows evaluation of HPTS environments. By frequency labeling the spins on specific HPTS hydrogen atoms, NMR NOESY follows the spin population transfer from one atom to another in close proximity, showing when atoms are near to each other.²⁸ Previous reports^{29–32} have demonstrated NMR NOE as an effective method to identify interactions of small molecules with micelles.

Through 2D NOESY experiments, we measured the interaction of protons in HPTS with protons in RMs. Figure 4 shows many cross peaks in the 2D NOESY spectrum of

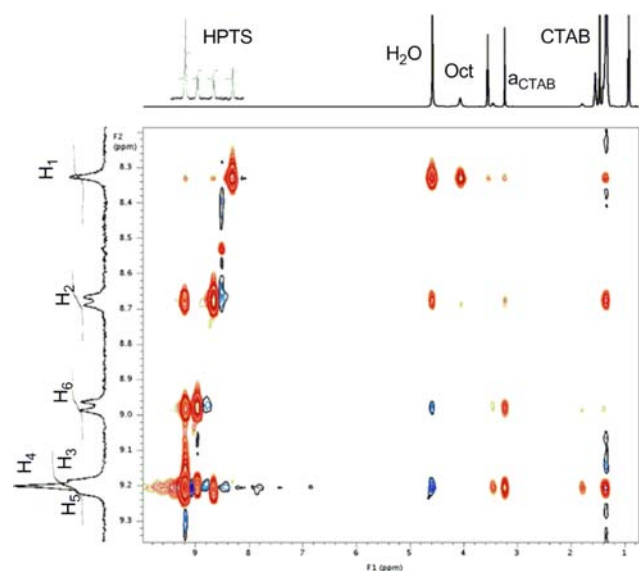


Figure 4. 2D NOESY spectrum showing interactions between HPTS with $w_0 = 10$ CTAB RM solution. Orange indicates positive peaks; blue indicates negative peaks. Note that the diagonal peaks are orange. The F2 axis is along the vertical or left side of the spectrum.

HPTS in the same $w_0 = 10$ CTAB RMs used for ultrafast transient absorption measurements. The off-diagonal or cross peaks, arise from intra- and intermolecular interactions. The HPTS NMR signals from protons on aromatic groups appear from ~ 8.3 to 9.3 ppm and are well separated from all the peaks associated with the RM, that is, water, CTAB surfactant, 1-octanol cosurfactant and cyclohexane. Figure 4 near 8.3 ppm on the F2 axis shows cross peaks arising from the interaction of HPTS H_1 with (right to left) H-atoms of the CTAB H_d /1-octanol H_δ , 1-octanol H_ω , CTAB headgroup H_a , 1-octanol OH, and water (following the numbering given in Figure 1). Strong interactions also appear for $F_2 \approx 9.2$ ppm (HPTS $H_3/H_4/H_5$) with CTAB H_d /1-octanol H_δ , CTAB H_c , H_a , H_b , and with water. Near 9.0 ppm the HPTS H_6 displays strong cross peaks with CTAB H_a and water, and weaker signals with CTAB H_d /1-octanol H_δ , and CTAB H_b and H_c . Finally HPTS H_2 signals near 8.7 ppm on F2 show strong interactions with CTAB H_d /1-

octanol H_δ , and water, and weaker interactions with H_a and 1-octanol OH. To generate these correlations, the HPTS would need to reside embedded in the CTAB RM interface, potentially as drawn in Figure 5.

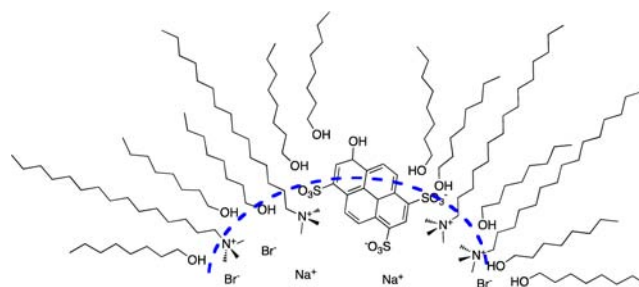


Figure 5. Cartoon suggesting a possible orientation of HPTS embedded in the CTAB/1-octanol RM interface that would lead to the observed time-resolved spectroscopy and NOESY results.

Corresponding 2D NMR experiments on AOT (see Supporting Information) showed only intramolecular interactions between HPTS protons as well as cross peaks reflecting intermolecular interactions between HPTS and water protons. No cross peaks were observed between HPTS and AOT or cyclohexane protons. These results demonstrate that HPTS does not interact with the protons forming the interface of the AOT RMs. Instead, HPTS resides well separated from the amphiphiles at the interface.

The sign of the NOE reflects the correlation time for the molecules and/or supramolecular structures giving rise to the NMR signals therefore suggesting the orientation of the HPTS at the CTAB RM interface. The H_1/H_2 HPTS/water interactions lead to a positive signal (same sign as diagonal peaks), while a negative signal (opposite sign from diagonal peaks) arises between water and HPTS $H_3/H_4/H_5/H_6$. This shows slower relaxation dynamics contributing to the H_1/H_2 NOEs compared to the $H_4/H_5/H_6$ signals, and consistent with a dramatic difference in the environments sampled by protons on different sides of the HPTS molecule.

Results from our NMR experiments corroborate and explain observations from ultrafast time-resolved absorption measurements. In CTAB RMs, HPTS molecules display no deprotonation and slow molecular reorientation. For the same samples, NOESY data show clear interactions of HPTS with water and the CTAB and 1-octanol, molecules comprising the RM interface. Embedding the HPTS molecule into the interface could present an environment that damps the photoinduced deprotonation reaction. Increased acidity reported at RM interfaces^{33–35} could also favor protonated HPTS but would not lead to the strong interactions between HPTS and molecules of the interface. The signs of the NOE signal for HPTS interactions with water reflect the substantially different correlation times for water sensed by HPTS protons H_1/H_2 compared to $H_3/H_4/H_5/H_6$ and are consistent with the HPTS oriented partially buried in the interface, as shown in Figure 5. The negative cross peaks indicate much shorter correlation times for the $H_4/H_5/H_6$ interactions than for H_1/H_2 . We assign the positive cross peaks to the OH groups at the water/surfactant interface; negative cross peaks are consistent with the bulk-like water in the interior of the RM. Halliday et al. recently reported distinct NMR signals from the OH groups in water and pentanol in CTAB/pentanol RMs³⁵ which we have also observed. This contrasts observations for bulk aqueous

solutions where signals coalesce because of the rapid chemical exchange. Considering the positive and negative NOE signals shown in Figure 4, we propose that the HPTS molecule is partially buried in the interface, as depicted in Figure 5, possibly due to the Coulomb attraction between the negatively charged SO_3^- groups on HPTS with the positively charged CTAB headgroups. It may seem unlikely to find a highly charged molecule like HPTS buried in the RM interface. However, through NMR NOE measurements, we demonstrated the $\text{VO}_2(\text{dipic})^-$ molecule comfortably embedded in AOT RM interfaces.³² Likewise, Binks et al. have observed interactions between the bipyridyl groups of the $\text{Ru}(\text{II})(\text{bpy})_3^{2+}$ molecule with AOT methyl protons.³⁶ In contrast, HPTS in AOT RMs behaves much like it does in bulk aqueous solution. That is, we observe no HPTS interactions with surfactant protons in the AOT RM interface and only negative NOE signals indicating that HPTS interacts with bulk-like water in the RM core. Ultrafast anisotropy measurements agree and indicate HPTS molecules in AOT RMs reside separated from the interface, well solvated by the RM water pool. This most likely reflects Coulomb repulsion between SO_3^- groups on both HPTS and the AOT headgroups. More extensive results from experiments probing a range of w_0 values and changes in other parameters will be forthcoming.

Our results demonstrate how complementary methods lead to detailed understanding of probe environment. Ultrafast time-resolved transient absorption measurements of HPTS in CTAB RMs show unequivocally that the environment impacts the dynamics, but do not reveal specific structures leading to the observed effects. Likewise, NOESY NMR measurements reveal details about the interaction of HPTS and RM components, but do not determine the HPTS proton transfer reaction kinetics. Combining ultrafast optical spectroscopy with various NMR studies results in a detailed explanation about the system and uncovers fundamental structural features that lead to observed dynamics. This marriage of methods provides the opportunity to measure complex systems over an incredible time range from femtoseconds to seconds, potentially connecting the highly dynamic regime with equilibrium processes.

■ ASSOCIATED CONTENT

📄 Supporting Information

Materials and methods, NOE spectrum for AOT RM, 1D and 2D NMR spectra of RM samples. This material is available free of charge via the Internet at <http://pubs.acs.org>.

■ AUTHOR INFORMATION

Corresponding Author

nancy.levinger@colostate.edu

Present Address

†JILA, 440 UCB, University of Colorado, Boulder, CO 80309-0440

Notes

The authors declare no competing financial interest.

■ ACKNOWLEDGMENTS

This material is based upon work supported by the National Science Foundation under grant 0628260.

■ REFERENCES

- (1) Thompson, W. H. In *Annu. Rev. Phys. Chem.*; Leone, S. R., Cremer, P. S., Groves, J. T., Johnson, M. A., Eds.; 2011; Vol. 62, p 599.
- (2) Kreuer, K. D. *Chem. Mater.* **1996**, *8*, 610.
- (3) Michel, H.; Behr, J.; Harrenga, A.; Kannt, A. *Annu. Rev. Biophys. Biomol. Struct.* **1998**, *27*, 329.
- (4) Wraight, C. A. *Biochim. Biophys. Acta-Bioenerg.* **2006**, *1757*, 886.
- (5) Spry, D. B.; Fayer, M. D. *J. Phys. Chem. B* **2009**, *113*, 10210.
- (6) Tielrooij, K. J.; Cox, M. J.; Bakker, H. J. *Chemphyschem* **2009**, *10*, 245.
- (7) Mondal, T.; Das, A. K.; Sasmal, D. K.; Bhattacharyya, K. *J. Phys. Chem. B* **2010**, *114*, 13136.
- (8) Sen Mojumdar, S.; Mondal, T.; Das, A. K.; Dey, S.; Bhattacharyya, K. *J. Chem. Phys.* **2010**, *132*, No. 19450510.1063/1.3428669.
- (9) Bardez, E.; Goguillon, B. T.; Keh, E.; Valeur, B. *J. Phys. Chem.* **1984**, *88*, 1909.
- (10) Pines, E.; Huppert, D.; Agmon, N. *J. Chem. Phys.* **1988**, *88*, 5620.
- (11) Tran-Thi, T. H.; Gustavsson, T.; Prayer, C.; Pommeret, S.; Hynes, J. T. *Chem. Phys. Lett.* **2000**, *329*, 421.
- (12) Roy, D.; Karmakar, R.; Mondal, S. K.; Sahu, K.; Bhattacharyya, K. *Chem. Phys. Lett.* **2004**, *399*, 147.
- (13) Ghosh, S.; Dey, S.; Mandal, U.; Adhikari, A.; Mondal, S. K.; Bhattacharyya, K. *J. Phys. Chem. B* **2007**, *111*, 13504.
- (14) Amdursky, N.; Orbach, R.; Gazit, E.; Huppert, D. *J. Phys. Chem. C* **2009**, *113*, 19500.
- (15) Cox, M. J.; Siwick, B. J.; Bakker, H. J. *Chemphyschem* **2009**, *10*, 236.
- (16) Barrash-Shiftan, N.; Brauer, B.; Pines, E. *J. Phys. Org. Chem.* **1998**, *11*, 743.
- (17) Hutter, T.; Presiado, I.; Ruschin, S.; Huppert, D. *J. Phys. Chem. C* **2010**, *114*, 2341.
- (18) Mukherjee, T. K.; Ahuja, P.; Koner, A. L.; Datta, A. *J. Phys. Chem. B* **2005**, *109*, 12567.
- (19) Barnadas-Rodriguez, R.; Estelrich, J. *J. Phys. Chem. B* **2009**, *113*, 1972.
- (20) Levinger, N. E.; Swafford, L. A. *Annu. Rev. Phys. Chem.* **2009**, *60*, 385.
- (21) De, T. K.; Maitra, A. *Adv. Colloid Interface Sci.* **1995**, *59*, 95.
- (22) Giustini, M.; Palazzo, G.; Colafemmina, G.; DellaMonica, M.; Giomini, M.; Ceglie, A. *J. Phys. Chem.* **1996**, *100*, 3190.
- (23) Zhu, D. M.; Feng, K. I.; Schelly, Z. A. *J. Phys. Chem.* **1992**, *96*, 2382.
- (24) Walde, P.; Giuliani, A. M.; Boicelli, C. A.; Luisi, P. L. *Chem. Phys. Lipids* **1990**, *53*, 265.
- (25) Spry, D. B.; Goun, A.; Glusac, K.; Moilanen, D. E.; Fayer, M. D. *J. Am. Chem. Soc.* **2007**, *129*, 8122.
- (26) Tokmakoff, A. *J. Chem. Phys.* **1996**, *105*, 1.
- (27) Cole, R. L.; Barisas, B. G.; Levinger, N. E. *Rev. Sci. Instrum.* **2010**, *81*, 093101.
- (28) Neuhaus, D.; Williamson, M. P. *The nuclear Overhauser effect in structural and conformational analysis*, 1st ed.; VCH: New York, 1989.
- (29) Bachofer, S. J.; Simonis, U.; Nowicki, T. A. *J. Phys. Chem.* **1991**, *95*, 480.
- (30) Sabatino, P.; Szczygiel, A.; Sinnaeve, D.; Hakimhashemi, M.; Saveyn, H.; Martins, J. C.; Van der Meeren, P. *Colloid Surf. A-Physicochem. Eng. Asp.* **2010**, *370*, 42.
- (31) Ceraulo, L.; Fanara, S.; Liveri, V. T.; Ruggirello, A.; Panzeri, W.; Mele, A. *Colloid Surf. A-Physicochem. Eng. Asp.* **2008**, *316*, 307.
- (32) Crans, D. C.; Rithner, C. D.; Baruah, B.; Gourley, B. L.; Levinger, N. E. *J. Am. Chem. Soc.* **2006**, *128*, 4437.
- (33) Baruah, B.; Roden, J. M.; Sedgwick, M.; Correa, N. M.; Crans, D. C.; Levinger, N. E. *J. Am. Chem. Soc.* **2006**, *128*, 12758.
- (34) Sedgwick, M. A.; Crans, D. C.; Levinger, N. E. *Langmuir* **2009**, *25*, 5496.
- (35) Halliday, N. A.; Peet, A. C.; Britton, M. M. *J. Phys. Chem. B* **2010**, *114*, 13745.
- (36) Binks, D. A.; Spencer, N.; Wilkie, J.; Britton, M. M. *J. Phys. Chem. B* **2010**, *114*, 12558.